Author Manuscript

Author Manuscript

Author Manuscript

Author Manuscript

HHS Public Access

Author manuscript

Cancer Discov. Author manuscript; available in PMC 2015 August 10.

Published in final edited form as:

Cancer Discov. 2012 January ; 2(1): 47–55. doi:10.1158/2159-8290.CD-11-0208.

Molecular ontogeny of donor-derived follicular lymphomas occurring after hematopoietic cell transplantation

Oliver Weigert[1], **Nadja Kopp**[1], **Andrew A. Lane**[1], **Akinori Yoda**[1], **Suzanne E. Dahlberg**[2], **Donna Neuberg**[2], **Anita Y. Bahar**[4], **Bjoern Chapuy**[1], **Jeff L. Kutok**[5], **Janina Longtine**[4], **Frank C. Kuo**[4], **Terry Haley**[3], **Maura Salois**[3], **Timothy J. Sullivan**[3], **David C. Fisher**[1], **Edward A. Fox**[3], **Scott J. Rodig**[4], **Joseph H. Antin**[1], and **David M. Weinstock**[1]

[1]Department of Medical Oncology, Dana-Farber Cancer Institute and Harvard Medical School, Boston, MA, USA

[2]Department of Biostatistics and Computational Biology, Dana-Farber Cancer Institute and Harvard Medical School, Boston, MA, USA

[3]Department of Microarray Core, Dana-Farber Cancer Institute and Harvard Medical School, Boston, MA, USA

[4]Department of Pathology, Brigham and Women's Hospital, Boston, MA, USA

[5]Infinity Pharmaceuticals, Cambridge, MA, USA

Abstract

The relative timing of genetic alterations that contribute to follicular lymphoma (FL) remains unknown. We analyzed a donor-recipient pair who both developed grade 2/3 FL seven years after allogeneic transplantation and donor lymphocyte infusions (DLI). Both FLs harbored identical *BCL2/IGH* rearrangements also present in 1-in-2000 cells in the DLI, and the same *V(D)J* rearrangement, which underwent somatic hypermutation both before and after clonal divergence. Exome sequencing of both FLs identified 15 shared mutations, of which 14 (including alterations in EP300 and KLHL6) were recovered from the DLI by ultra-deep sequencing (average read coverage, 361,723), indicating acquisition at least 7 years prior to clinical presentation. Six additional mutations were present in only one FL and not the DLI, including an ARID1A premature stop, indicating later acquisition during clonal divergence. Thus, ultra-sensitive sequencing can map clonal evolution within rare subpopulations during human lymphomagenesis *in vivo*.

Significance—For the first time, we define the molecular ontogeny of follicular lymphoma during clonal evolution *in vivo*. Using ultra-sensitive mutation detection, we mapped the time-course of somatic alterations after passage of a malignant ancestor by hematopoietic cell transplantation.

Corresponding author: Dr. David Weinstock, Dana-Farber Cancer Institute, 450 Brookline Avenue, Dana 510B, Boston, MA 02215. Phone: 617 632-4245; Fax: 617 632-5167; dweinstock@partners.org (contact for reprint request).

Disclosure: The authors have no competing financial interests to disclose and the material has not been published or presented elsewhere.

Author Manuscript Author Manuscript Author Manuscript Author Manuscript

Keywords

follicular lymphoma; bone marrow transplantation; lymphomagenesis; deep sequencing

Introduction

Follicular lymphoma (FL) is the most common non-Hodgkin lymphoma (NHL) in North America (1) and usually follows an indolent clinical course, with 10-year survival rates ranging from 36-71% (2). The molecular hallmark of FL is rearrangement of chromosome 18q21, which results in overexpression of the anti-apoptotic protein BCL2, most commonly through juxtaposition to the immunoglobulin heavy chain (*IGH*) locus (3). Up to 25% of healthy individuals have circulating *BCL2/IGH*-harboring cells (4, 5), yet FL is diagnosed in only 1 out of 24,000 persons in the United States annually (6). This suggests that additional genetic alternations are required for lymphomagenesis. Recurrent mutations have been identified in FL (7-10), but their timing during lymphomagenesis remains unknown.

Donor-derived malignancies after hematopoietic cell transplantation are rare (11) but provide unique models for assessing clonal evolution of human tumors *in vivo*. Previous reports of donor-derived malignancies have lacked detailed molecular analysis. We performed ultra-sensitive mutation detection to define *in vivo* clonal diversification in paired FLs from a donor-recipient sibling pair who presented more than 7 years after hematopoietic cell transplantation and subsequent donor lymphocyte infusions (DLI).

Results

A 41-year old woman was found to have asymptomatic leukocytosis and was diagnosed with chronic-phase chronic myeloid leukemia (CML) in 1999. In June 2000, she received myeloablative conditioning followed by transplantation of unmanipulated bone marrow from her 40-year old HLA-identical sister (Figure 1A). She received methotrexate and tacrolimus as graft-versus-host-disease (GvHD) prophylaxis and achieved a complete hematological remission, but BCR/ABL1 transcript remained detectable by PCR. Peripheral blood leukocytes were collected from her donor in 3/2002 and donor leukocyte infusions (DLI) were prepared by Ficoll separation. She received three DLI to a total of 1.45×10^8 cells/kg, with the last in June 2002. She remained PCR positive for BCR/ABL1 with no evidence of GVHD. She initiated interferon alpha-2a in 2004, which resulted in a complete molecular remission for two years. In 2006, she became PCR positive and was switched to imatinib, which again resulted in a complete molecular remission (Figure 1A).

In November 2009, the donor presented with palpable cervical lymphadenopathy and right leg edema. Imaging demonstrated widespread lymphadenopathy and soft tissue masses. Biopsy of a right inguinal lymph node and bone marrow revealed grade 2 follicular lymphoma with focal areas of grade 3A (Figure 1B). Six months later, the recipient developed shortness of breath. Imaging demonstrated pleural and peritoneal effusions, as well as extensive lymphadenopathy. Biopsy of a left inguinal lymph node and bone marrow also revealed grade 2 follicular lymphoma with focal areas of grade 3A and no evidence of CML (Figure 1B). Morphologic and immunohistochemical findings in both FLs were highly

Author Manuscript Author Manuscript Author Manuscript Author Manuscript

similar, with both cases infiltrated by tumor cells expressing CD20, CD10, BCL2 and BCL6 (Figure 1B).

The morphological similarity between the lymphomas and their virtually synchronous timing suggested that a common FL ancestor was passed from the donor to the recipient. PCR with primers overlapping the major breakpoint region of *BCL2* and a VH3 consensus sequence amplified identical *BCL2/IGH* rearrangements from the donor's FL and the recipient's FL (Figure 2A-B). Thus, the two lymphomas were derived from a common ancestral population that harbored *BCL2/IGH*. PCR with the same primers identified an identical product from the DLI, the most recently passed specimen from donor to recipient (Figure 2A-B). This indicates that transplantation of *BCL2/IGH*-harboring cells occurred at least 7 years prior to FL presentation.

To determine the frequency of *BCL2/IGH*-positive cells in the DLI, we assayed *BCL2/IGH* by quantitative PCR (qPCR). The fraction of DLI cells harboring *BCL2/IGH* was approximately 1-in-2000 (0.026% of *GAPDH* alleles) (Figure 2C). The cleavage and repair that mediate *BCL2/IGH* translocation are thought to involve the V(D)J recombinase RAG1/2 (12), which is expressed in immature lymphocyte progenitors. We utilized the pan-B-cell marker CD19 to sort positive and negative populations from the DLI by flow cytometry (Figure S1). As expected, the *BCL2/IGH* rearrangement was below the level of detection in the CD19-negative subset of the DLI, either by conventional PCR (Figure 2A) or by qPCR (lower limit of sensitivity ∼1-in-25,000 cells) (Figure S1).

Follicular lymphomas typically harbor completed *IGH* rearrangements (3). We performed multiplex PCR for the detection of clonal *IGH* rearrangements, as previously described (13). Both lymphomas harbored identically-sized rearrangements that utilized the same *VH*, *DH* and *JH* segments and shared identical non-templated insertions (Figure 2D), indicating that the common FL ancestor had completed *IGH* rearrangement.

FL is characterized by ongoing somatic hypermutation, a response to antigen stimulation within the germinal center. To identify single nucleotide variants (SNVs) and small insertions/deletions (InDels) consistent with somatic hypermutation, we compared the clonal *IGH* rearrangements from both FLs to the donor's germline *VH3-66* segment that was involved in the *IGH* rearrangement. There were multiple identical somatic alterations within the amplified region present in both FLs (Figure 2D), indicating that the common ancestor had initiated somatic hypermutation. Both FL-derived *IGH* rearrangements also harbored distinct somatic alterations, consistent with ongoing somatic hypermutation during clonal divergence (Figure 2D).

The availability of both the donor's and recipient's FLs as well as a common ancestor population within the DLI offered a unique opportunity to delineate human lymphoma ontogeny. To identify shared and divergent genetic events, we performed exome sequencing of formalin-fixed paraffin-embedded samples of both FLs and a frozen aliquot of DLI. Annotated sequence variants were intersected, filtered, sorted and selected as outlined in the Supplement (Figures S2-3, Tables S1-2). All mutations were verified to be somatic by PCR and Sanger sequencing from both FLs and appropriate germline specimens (Table S3).

Author Manuscript Author Manuscript Author Manuscript Author Manuscript

Bioinformatic predictions of the functional impact for each somatic missense mutation are included in Table S4.

Overall, we recovered 12 coding SNVs and 2 coding InDels that were present in both lymphomas, 3 SNVs that were unique to the donor's FL, and 4 SNVs that were unique to the recipient's FL (Table 1). None of the mutations were detected within the DLI by Sanger sequencing. In addition, for the 4 SNVs unique to the recipient's FL, we excluded a germline polymorphism by comparison with the recipient buccal swab.

Among the identical SNVs in both FLs were two in BCL2, which is known to be a target of aberrant somatic hypermutation in FL (Figure 3A) (14). Based on sequencing of cDNA from the recipient's FL, both SNVs were present in 100% of BCL2 transcript (Figure 3A), indicating that the mutations are present in *cis* on the translocated allele. An in-frame deletion in EP300, an acetyltransferase that is recurrently mutated in FL and diffuse large B-cell lymphoma (DLBCL) (7), was present in both FLs (Figure 3B). In addition, we identified an in-frame insertion in KLHL6 (Figure 3B), which was recently found to be mutated in chronic lymphocytic leukemia (CLL) (15), DLBCL and FL (10).

Among the SNVs unique to the recipient's FL was an R1276 premature stop mutation in ARID1A (adenine-thymine (AT)-rich interactive domain-containing protein 1A) (Figure 3C) that was previously reported in pancreatic cancer (16). The *ARID1A* locus is within a region of chr. 1p that is deleted in approximately 20% of FL cases, and deletion is linked to inferior prognosis (17). Although the premature stop mutation was present only in the recipient's FL, both lymphomas had reduced BAF250 (the protein product of *ARID1A*) expression by immunohistochemical analysis (Figures 3E and S4B). To determine whether ARID1A expression could be affected by copy number loss in the donor's FL, we performed qPCR on genomic DNA from both FLs, as well as control samples. As outlined in Figure 3D, qPCR identified copy number loss (copy number, 1.84; p=0.022 compared to donor germline) at this locus in the donor's FL but not the recipient's FL (Figure 3D).

Exome sequencing technology currently lacks adequate sensitivity to identify very rare events, such as those occurring in 1-in-2,000 cells. To determine whether the somatic mutations that we identified are present at a low frequency within the DLI, we PCR amplified regions flanking each mutation site from the DLI and subjected the products to ultra-sensitive deep sequencing (average read coverage at mutation site, 361,723; range, 16,684–1,169,555). To correct for background frequencies of non-germline calls, we PCR amplified and deep sequenced the same positions from the donor buccal swab (average read coverage at the mutation site, 418,499; range, 20,711–1,070,734). Mutations categorized as unique to one FL were also PCR amplified from the other FL and deep sequenced in parallel.

Eleven of the 12 SNVs and the 2 InDels that were identified in both FLs were ‘enriched’ in the DLI, *i.e.*, recovered at frequencies significantly above background (Table 1). Thus, those mutations were acquired more than 7 years prior to presentation of either FL. All 4 SNVs unique to the recipient's FL and the RFTN1 V254M mutation identified only in the donor's FL were not enriched in the DLI or the other FL, consistent with subsequent acquisition

Author Manuscript Author Manuscript Author Manuscript Author Manuscript

during clonal divergence. RFTN1 (raftlin linking protein 1) is required for the integrity of lipid rafts in B-cells and regulates B-cell receptor signaling (18). Recurrent mutations in close proximity to RFTN1 V254 were recently reported in DLBCL (10).

Of the final two mutations, ATP6V1B2 R400Q (Figure 3D) was detected only in the donor's FL but was enriched in the DLI. CTSS M185V (Figure 3D) was initially detected only in the donor's FL, but deep sequencing recovered the mutation in 4.7% of reads from the recipient's FL and demonstrated enrichment in the DLI (Table 1).

Discussion

The presentation of virtually synchronous follicular lymphomas in a donor-recipient pair many years after hematopoietic cell transplantation provided the opportunity to interrogate clonal evolution in separate hosts. We demonstrate that the same *BCL2/IGH* rearrangement in both FLs was also present within the DLI passed from donor to recipient 7 years prior to FL presentation. The *BCL2/IGH*-harboring cells within the DLI were derived from a common ancestor, have undergone the germinal center reaction, and are capable of initiating FL with a surprisingly similar latency.

BCL2/IGH-harboring cells were present at a frequency of 1-in-2,000 within the DLI. This high frequency suggests that the *BCL2/IGH*-harboring cells had a survival advantage within the donor more than 7 years prior to lymphoma presentation. Based on a frequency of 1-in-2000 cells, more than 4 million potential FL precursors were transferred within the DLI from the donor to the recipient. The true number of transplanted FL precursors may have been higher for two reasons. First, *BCL2/IGH*-harboring cells could have been present in the original bone marrow transplant, which was not available for analysis. Second, it is possible that somatic hypermutation affected the primer sites we utilized for qPCR quantification of *BCL2/IGH* in some or all of the *BCL2/IGH*-rearranged cells.

To identify markers of convergent and divergent clonal evolution within the two FLs, we performed exome sequencing. Previous efforts at exome sequencing have primarily used high-quality DNA from fresh or fresh-frozen tissues and cell suspensions with high tumor cell content (10, 15). In contrast, the DNA available for our study was isolated from FFPE tissue with only moderate lymphoma cell infiltration (∼40-45% and 60-65% for the donor's and recipient's FL, respectively (Figure S4A)). The number of coding SNVs in a recent study of non-Hodgkin lymphomas ranged from 20-135 per genome (10). As we identified fewer than 20 coding SNVs per FL, it is likely that additional mutations were present but not recovered. The recovery and validation rates in our study, although within previously reported ranges (19, 20), were likely reduced compared with recent comprehensive analyses of B-cell lymphoma (7, 10), because of the use of FFPE-derived specimens with limited tumor cell infiltration. Nonetheless, the cohort of mutations we identified was sufficient to track the acquisition of somatic SNVs and InDels within FL ancestors over several years prior to clinical presentation.

Among the mutations present in both FLs and the DLI was a novel in-frame insertion in exon 6 of KLHL6, downstream of the SNVs recently described in CLL (15) and non-

Author Manuscript Author Manuscript Author Manuscript Author Manuscript

Hodgkin lymphoma (10). KLHL6 is a lymphoid-tissue specific BTB-kelch protein that is highly expressed in germinal center B-cells and involved in B-cell receptor signaling (21). We also recovered a novel in-frame deletion in the bromodomain of EP300, an acetyltransferase involved in transcriptional activation of p53 and inactivation of BCL6 (7). Disruption of EP300 or its partners CREBBP and MEF2B occurs in more than 50% of FL cases (7, 22). Our data indicate that the EP300 mutation was acquired several years prior to FL onset, raising the possibility that acetyltransferase alterations can be early oncogenic events.

Loss-of-function mutations in ARID1A/BAF250, a putative tumor suppressor gene, are present in approximately 60% of ovarian clear cell carcinoma, 30% of endometroid carcinomas (23, 24) and other epithelial tumors, but have not been reported in hematologic malignancies yet. Of note, the *ARID1A* locus is within a commonly deleted region on chr. 1p within close proximity to *TNFRSF14*, which is recurrently mutated in FL (9). We demonstrate that the recipient's lymphoma acquired a premature stop codon mutation in ARID1A that could not be retrieved from the donor's lymphoma or the DLI, suggesting a later event in lymphomagenesis. Interestingly, both lymphomas showed reduced ARID1A/BAF250 protein staining, suggesting alternative mechanisms of ARID1A inactivation. Based on the frequency of variant reads at SNV sites from exome sequencing (Table 1), the donor's FL specimen contained approximately 45% tumor cells. Staining of the tumor for CD10-positive cells was consistent with this estimate (Figure S4A). Thus, we would expect single allele loss to result in a copy number of approximately 1.55. The difference between 1.55 and the measured allele frequency in the donor's FL (1.84) could indicate that *ARID1A* allele loss was limited to a subpopulation of the donor's FL or it could simply reflect the limit of precision for this assay.

The ATP6V1B2 R400Q mutation was enriched in the DLI but only present in the donor's FL. Similarly, CTSS M185V was present in the DLI, the donor's FL, but only a small subset of recipient FL cells. These findings are consistent with at least two scenarios. First, the recipient's FL could be derived from a clonally diversified population of ancestor cells transferred from the donor. A second possibility is that the mutant allele was lost during clonal evolution in some (CTSS M185V) or all (ATP6V1B2 R400Q) of the FL cells within the recipient. Loss of a mutant allele would suggest that the allele is a passenger rather than a driver of lymphomagenesis.

The donor and recipient lymphomas presented after a long but surprisingly similar latency despite marked differences in immune competence between the host and recipient. A previous report identified donor-derived mantle cell lymphomas diagnosed virtually simultaneously in donor and recipient 12 years after transplantation (25). Similar latency in donor and recipient lymphomas could indicate that host immunity plays a limited role in restraining the expansion of some FL and mantle cell lymphomas. Previous studies have demonstrated that prognosis among patients with FL correlates with transcriptional signatures derived from infiltrating, nonmalignant T-cells, macrophages and dendritic cells (26). Therefore, the pace of disease expansion may to some extent be separable from prognosis if immune competence affects the latter but not the former.

Author Manuscript Author Manuscript Author Manuscript Author Manuscript

In conclusion, we utilized ultra-sensitive mutation detection to elucidate the molecular ontogeny of follicular lymphoma during clonal evolution in separate hosts. The same approach has broad applicability for identifying genetic variants within pooled tumor populations that confer subsequent phenotypes, including therapeutic resistance and metastatic potential.

Materials and Methods

The study was approved by the Dana-Farber Cancer Institute Institutional Review Board and both participants gave written informed consent. Additional description of methods is included in the Supplementary Material.

Nucleic Acids Nucleic Acids were isolated from formalin-fixed paraffin embedded (FFPE) lymph node biopsies of both lymphomas and residual aliquots of the fresh frozen DLI, germline DNA of both patients was isolated from buccal swabs (Qiagen, USA).

Immunohistochemistry was performed on 5 μm FFPE tissue sections using the following primary antibodies: anti-CD20 (RTU, clone L26, DAKO), anti-CD10 (1:80 dilution, clone 56C6, Novocastra/Leica Microsystems, Wetzler, Germany), anti-BCL6 (1:100 dilution, cat. sc-858, Santa Cruz Biotechnology, Santa Cruz, CA), anti-BCL2 (1:1000 dilution, cat. M0887, DAKO), and anti-ARID1A/BAF250A (1:50 dilution, cat. sc-32761, Santa Cruz Biotechnology, Santa Cruz, CA (Figure 3E); 1:150 dilution, cat. HPA005456, Sigma-Aldrich, St. Louis, MO (Figure S4B)).

Real-time Quantitative PCR

(TaqMan, Applied Biosystems) for BCL2/IGH and GAPDH was performed in triplicate and repeated on separate dates. A translocation specific probe was utilized that hybridizes to the junction region. Standard curves were generated using serial dilutions of cloned BCL2/IGH and GAPDH PCR products and analyzed according to published guidelines (27). Refer to Supplementary Methods for details.

Flow Cytometry Sorting

The DLI sample was stained for CD19 (PE-Cy7 anti-CD19, clone HIB19, BD Pharmingen) and sorted (BD ARIA II SORP Sorter, BD Biosciences). Post-sorting analysis demonstrated 98.1% (CD19 positive) and 99.8% (CD19 negative) pure populations (Figure S1), respectively, and genomic DNA was extracted using DNA Blood Mini kit (Qiagen, USA).

Duplex Real-Time PCR Copy Number (CN) Assay

(TaqMan Genotyping Master Mix, Applied Biosystems) was performed using genomic DNA from both FLs and germline samples using FAM-labeled ARID1A CN Assay (HS02336512_cn, Applied Biosystems) and VIC/TAMRA-labeled RNaseP CN Reference Assay (Applied Biosystems) according to the manufacturer's recommentations (7500 Real-Time PCR System, Applied Biosystems) and analyzed with CopyCaller Software (version 1.0, Applied Biosystems).

Author Manuscript Author Manuscript Author Manuscript Author Manuscript

Exome Sequencing

Genomic DNA from both FLs and the DLI were subjected to exome sequencing (SOLiD4 instrument, Life Technologies; SureSelect Target Enrichment System for the Applied Biosystems SOLiD system reagents, Applied Biosystems) to a mean depth of 33.2 and 34.2. Details are provided in the Supplementary Methods (Tables S1-2, Figures S2-3). Mutations confirmed to be somatic by PCR and Sanger sequencing in both FLs, the DLI and appropriate germline samples were considered candidates for further analysis and experiments (Table S3).

We utilized the frequency of variant calls at somatic SNVs to estimate the extent of tumor cell infiltration. Among SNVs with a coverage of at least 10 reads at this position, the mean frequency of variant calls was 22.4% for the donor FL and 31.6% for the recipient FL. Thus, based on exome sequencing, the lymphoma cell infiltration can be estimated to be 44.8% (FL donor) and 63.2% (FL recipient).

PCR and Sanger sequencing

PCR primers were designed using Primer3 (28) (version 0.4.0, http://frodo.wi.mit.edu/primer3/) and primer sequences are provided in Table S5. Sanger sequencing was performed at the Dana Farber Cancer Institute Molecular Biology Core Facilities and the Dana-Farber/Harvard Cancer Center DNA Sequencing Facility.

Ultra-deep sequencing of PCR products and computational analysis

Somatic sequence variants shared by both lymphomas or unique to one lymphoma were amplified by PCR (KOD Xtreme™ Hot Start DNA Polymerase, Novagen) from genomic DNA of the DLI, both FLs, and the donor's buccal swab. PCR products overlapping the same region were divided into separate pools. Library construction from the PCR products was carried out using the Amplicon Concatenation Protocol for the Applied Biosystems SOLiD system (Life Technologies). A library was constructed from each of two aliquots from each sample, and barcoded for multiplexing. Briefly, 500ng of pooled PCR products were concatenated using T4 ligase, sheared to approximately 150 base pairs, ligated to adapters, and amplified by PCR. Barcoded libraries were then mixed and the mixture sequenced on each of two slides. Use of two aliquots of each PCR pool served as a technical replicate for library construction; sequencing the mixtures on two slides served as a technical replicate for the sequencing. Approximately 50 bases from one end of each fragment were sequenced using the SOLiD 4 instrument and reagents.

Resulting data was mapped to a single, custom reference generated to include all fragment sequences using either mapreads or BFAST, for single nucleotide variant and InDel detection, respectively. For both analyses, each observed substitution or InDels was tallied by position and strand across the sequence using Samtools v.0.1.12a. In order to correct for erroneous misincorporations by sequencing and positional bias, the lesser of the stranded tallies were taken as the coverage.

Statistical Analysis of targeted deep sequencing was performed by calculating the relative mutation frequency (*f*) for each candidate gene, assuming that the number of mutations

Author Manuscript Author Manuscript Author Manuscript Author Manuscript

follows a Poisson distribution. We tested the null hypotheses that the mutation rate ratio between DLI and germline ($f_{DLI}/f_{germline}$) was equal to 1 for each comparison. We analyzed the DLI as it represents the most recently passed specimen from donor to recipient. The Bonferroni adjusted two-sided p-value of 0.00238 (= 0.05/21) was the level determining statistical significance.

Supplementary Material

Refer to Web version on PubMed Central for supplementary material.

Acknowledgments

We thank Jon Aster and Margaret Shipp for thoughtful review.

Financial support: O.W. is supported by the Deutsche Forschungsgemeinschaft. J.H.A is supported by the Jock and Bunny Adams Education and Research Endowment. D.M.W. is supported by a Stand Up To Cancer Innovative Research Grant, an American Cancer Society Research Scholar Grant and the Stellato Fund.

References

1. Anderson JR, Armitage JO, Weisenburger DD. Epidemiology of the non-Hodgkin's lymphomas: distributions of the major subtypes differ by geographic locations. Non-Hodgkin's Lymphoma Classification Project. Ann Oncol. 1998; 9:717–20. [PubMed: 9739436]
2. Solal-Celigny P, Roy P, Colombat P, White J, Armitage JO, Arranz-Saez R, et al. Follicular lymphoma international prognostic index. Blood. 2004; 104:1258–65. [PubMed: 15126323]
3. Swerdlow, SH.; Campo, E.; Harris, NL.; Jaffe, ES.; Pileri, SA.; Stein, H., et al. WHO Classification of Tumours of Haematopoietic and Lymphoid Tissues. 4. Lyon: IARC; 2008.
4. Summers KE, Goff LK, Wilson AG, Gupta RK, Lister TA, Fitzgibbon J. Frequency of the Bcl-2/IgH rearrangement in normal individuals: implications for the monitoring of disease in patients with follicular lymphoma. J Clin Oncol. 2001; 19:420–4. [PubMed: 11208834]
5. Roulland S, Navarro JM, Grenot P, Milili M, Agopian J, Montpellier B, et al. Follicular lymphoma-like B cells in healthy individuals: a novel intermediate step in early lymphomagenesis. J Exp Med. 2006; 203:2425–31. [PubMed: 17043145]
6. Staudt LM. A closer look at follicular lymphoma. N Engl J Med. 2007; 356:741–2. [PubMed: 17301308]
7. Pasqualucci L, Dominguez-Sola D, Chiarenza A, Fabbri G, Grunn A, Trifonov V, et al. Inactivating mutations of acetyltransferase genes in B-cell lymphoma. Nature. 2011; 471:189–95. [PubMed: 21390126]
8. Morin RD, Johnson NA, Severson TM, Mungall AJ, An J, Goya R, et al. Somatic mutations altering EZH2 (Tyr641) in follicular and diffuse large B-cell lymphomas of germinal-center origin. Nat Genet. 2010; 42:181–5. [PubMed: 20081860]
9. Cheung KJ, Johnson NA, Affleck JG, Severson T, Steidl C, Ben-Neriah S, et al. Acquired TNFRSF14 mutations in follicular lymphoma are associated with worse prognosis. Cancer research. 2010; 70:9166–74. [PubMed: 20884631]
10. Morin RD, Mendez-Lago M, Mungall AJ, Goya R, Mungall KL, Corbett RD, et al. Frequent mutation of histone-modifying genes in non-Hodgkin lymphoma. Nature. 2011
11. Sala-Torra O, Hanna C, Loken MR, Flowers ME, Maris M, Ladne PA, et al. Evidence of donor-derived hematologic malignancies after hematopoietic stem cell transplantation. Biol Blood Marrow Transplant. 2006; 12:511–7. [PubMed: 16635786]
12. Tsai AG, Lu H, Raghavan SC, Muschen M, Hsieh CL, Lieber MR. Human chromosomal translocations at CpG sites and a theoretical basis for their lineage and stage specificity. Cell. 2008; 135:1130–42. [PubMed: 19070581]

Author Manuscript Author Manuscript Author Manuscript Author Manuscript

13. van Dongen JJ, Langerak AW, Bruggemann M, Evans PA, Hummel M, Lavender FL, et al. Design and standardization of PCR primers and protocols for detection of clonal immunoglobulin and T-cell receptor gene recombinations in suspect lymphoproliferations: report of the BIOMED-2 Concerted Action BMH4-CT98-3936. Leukemia. 2003; 17:2257–317. [PubMed: 14671650]
14. Tanaka S, Louie DC, Kant JA, Reed JC. Frequent incidence of somatic mutations in translocated BCL2 oncogenes of non-Hodgkin's lymphomas. Blood. 1992; 79:229–37. [PubMed: 1339299]
15. Puente XS, Pinyol M, Quesada V, Conde L, Ordonez GR, Villamor N, et al. Whole-genome sequencing identifies recurrent mutations in chronic lymphocytic leukaemia. Nature. 2011
16. Forbes SA, Bindal N, Bamford S, Cole C, Kok CY, Beare D, et al. COSMIC: mining complete cancer genomes in the Catalogue of Somatic Mutations in Cancer. Nucleic Acids Res. 2011; 39:D945–50. [PubMed: 20952405]
17. O'Shea D, O'Riain C, Gupta M, Waters R, Yang Y, Wrench D, et al. Regions of acquired uniparental disomy at diagnosis of follicular lymphoma are associated with both overall survival and risk of transformation. Blood. 2009; 113:2298–301. [PubMed: 19141865]
18. Saeki K, Miura Y, Aki D, Kurosaki T, Yoshimura A. The B cell-specific major raft protein, Raftlin, is necessary for the integrity of lipid raft and BCR signal transduction. Embo J. 2003; 22:3015–26. [PubMed: 12805216]
19. Ley TJ, Mardis ER, Ding L, Fulton B, McLellan MD, Chen K, et al. DNA sequencing of a cytogenetically normal acute myeloid leukaemia genome. Nature. 2008; 456:66–72. [PubMed: 18987736]
20. Wilhelm BT, Briau M, Austin P, Faubert A, Boucher G, Chagnon P, et al. RNA-seq analysis of 2 closely related leukemia clones that differ in their self-renewal capacity. Blood. 2011; 117:e27–38. [PubMed: 20980679]
21. Kroll J, Shi X, Caprioli A, Liu HH, Waskow C, Lin KM, et al. The BTB-kelch protein KLHL6 is involved in B-lymphocyte antigen receptor signaling and germinal center formation. Mol Cell Biol. 2005; 25:8531–40. [PubMed: 16166635]
22. Morin RD, Mendez-Lago M, Mungall AJ, Goya R, Mungall KL, Corbett RD, et al. Frequent mutation of histone-modifying genes in non-Hodgkin lymphoma. Nature. 2011; 476:298–303. [PubMed: 21796119]
23. Wiegand KC, Shah SP, Al-Agha OM, Zhao Y, Tse K, Zeng T, et al. ARID1A mutations in endometriosis-associated ovarian carcinomas. N Engl J Med. 2010; 363:1532–43. [PubMed: 20942669]
24. Jones S, Wang TL, Shih Ie M, Mao TL, Nakayama K, Roden R, et al. Frequent mutations of chromatin remodeling gene ARID1A in ovarian clear cell carcinoma. Science. 2010; 330:228–31. [PubMed: 20826764]
25. Christian B, Zhao W, Hamadani M, Sotomayor EM, Navarro W, Devine SM, et al. Mantle cell lymphoma 12 years after allogeneic bone marrow transplantation occurring simultaneously in recipient and donor. J Clin Oncol. 2010; 28:e629–32. [PubMed: 20733121]
26. Dave SS, Wright G, Tan B, Rosenwald A, Gascoyne RD, Chan WC, et al. Prediction of survival in follicular lymphoma based on molecular features of tumor-infiltrating immune cells. N Engl J Med. 2004; 351:2159–69. [PubMed: 15548776]
27. van der Velden VH, Cazzaniga G, Schrauder A, Hancock J, Bader P, Panzer-Grumayer ER, et al. Analysis of minimal residual disease by Ig/TCR gene rearrangements: guidelines for interpretation of real-time quantitative PCR data. Leukemia. 2007; 21:604–11. [PubMed: 17287850]
28. Rozen S, Skaletsky H. Primer3 on the WWW for general users and for biologist programmers. Methods Mol Biol. 2000; 132:365–86. [PubMed: 10547847]

Abbreviations

CLL	chronic lymphocytic leukemia
CML	chronic myeloid leukemia
DLBCL	diffuse large B cell lymphoma

Author Manuscript Author Manuscript Author Manuscript Author Manuscript

DLI	donor lymphocyte infusion
FFPE	formalin-fixed, paraffin embedded
FL	follicular lymphoma
GvHD	graft-versus-host-disease
IGV	Integrated Genome Browser
IHC	immunohistochemistry
InDel	insertion/deletion
SNV	single nucleotide variation

Author Manuscript Author Manuscript Author Manuscript Author Manuscript

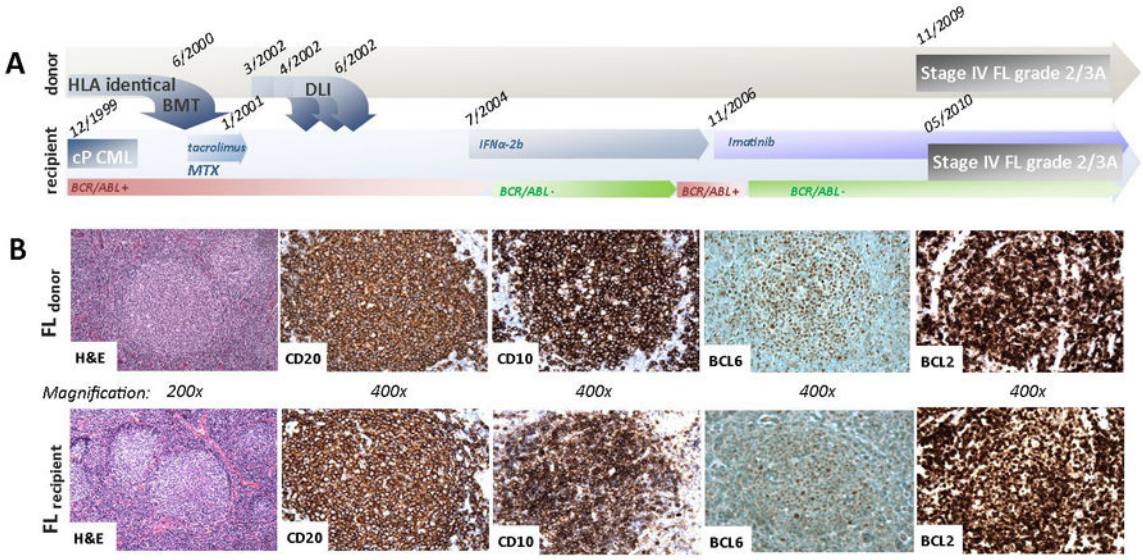

Figure 1.

Presentation of follicular lymphoma in the donor and recipient.

A. Time course of chronic phase CML (cP CML) in the recipient followed by bone marrow transplantation (BMT), administration of three donor lymphocyte infusions (DLI) and treatment for detectable BCR/ABL1 transcript by RT-PCR. Follicular lymphoma (FL) was diagnosed in both the donor and the recipient within a 6-month period. **B.** Immunohistochemistry with hematoxylin and eosin (H&E) or antibodies against the indicated markers.

Author Manuscript Author Manuscript Author Manuscript Author Manuscript

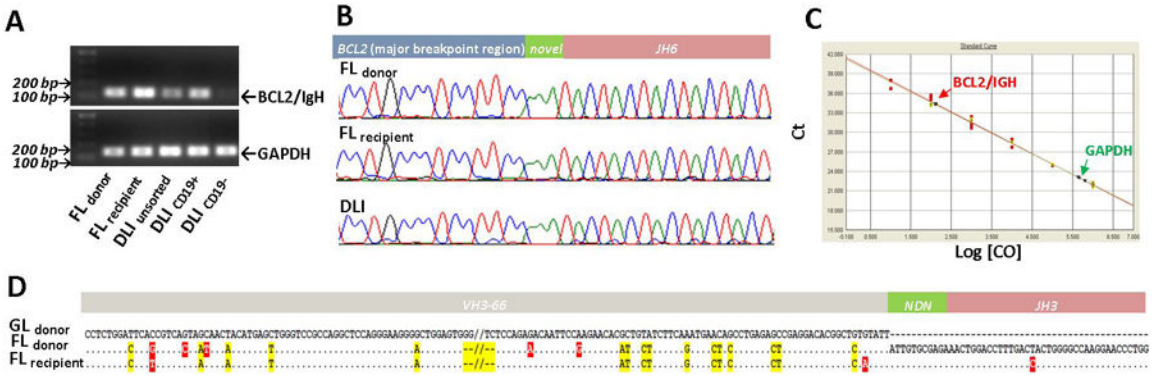

Figure 2.

Follicular lymphomas in the donor and recipient are derived from a common ancestor. **A.** PCR amplification of *IGH/BCL2* genomic DNA from both lymphomas, DLI, or flow-sorted DLI for CD19-positive and CD19-negative populations. Amplification of GAPDH DNA is shown as a control. **B.** Identical *BCL2/IGH* rearrangements amplified from genomic DNA from both lymphomas and DLI. **C.** Quantitative PCR with primer sets and probes for the patient specific *BCL2/IGH* junction or GAPDH. Standard curves were generated from cloned *BCL2/IGH* (in red) and GAPDH (in green) PCR products. Genomic DNA of the DLI was tested in triplicates and results were plotted against the standard curves. **D.** The same IGH rearrangement was amplified from both lymphomas. Germline (GL) VH3-66*4 was amplified from the donor's buccal swab and is shown for comparison. Mismatches that are shared between both lymphomas are in yellow. Mismatches unique to a single lymphoma are in red. '--//--' indicates a small deletion. 'NDN' indicates non-templated nucleotides flanking DH sequence.

Author Manuscript Author Manuscript Author Manuscript Author Manuscript

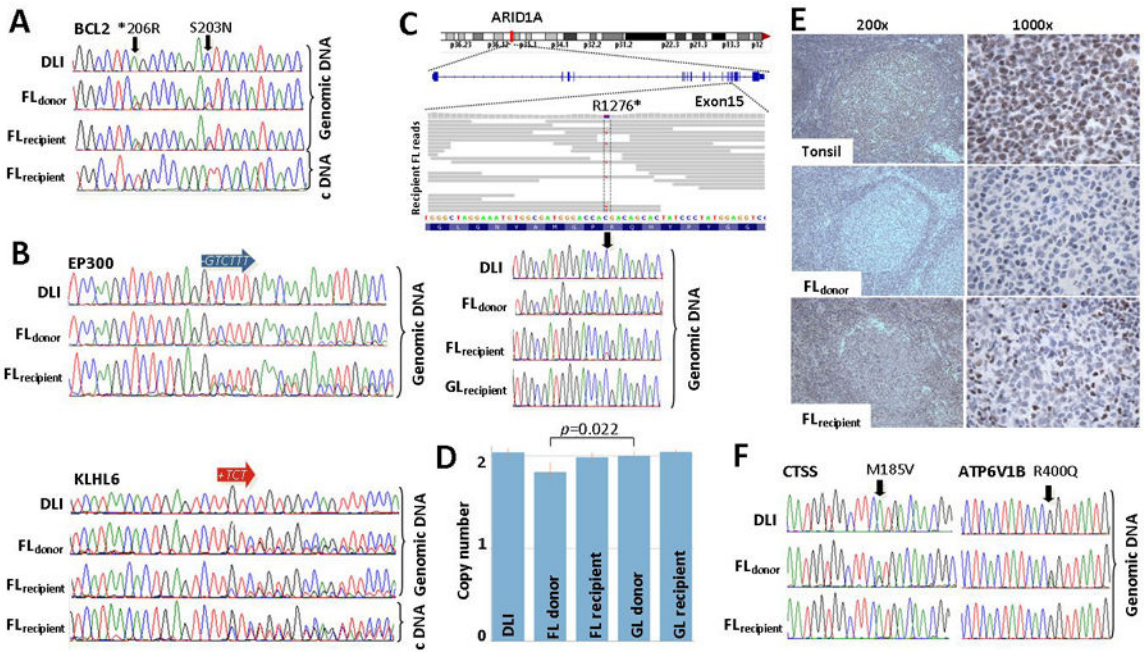

Figure 3.

Mutations in the paired follicular lymphomas.

A. Two SNVs were present in BCL2 in both FLs but not detectable by Sanger sequencing in the DLI. Only the mutant allele is present in cDNA from the recipient's FL. **B.** In-frame deletion in EP300 and in-frame insertion in KLHL6 were detectable by Sanger sequencing in both lymphomas. In contrast with BCL2, both the wild-type and mutated alleles of KLHL6 were expressed in the recipient FL. **C.** Exome sequencing reads spanning ARID1A R1276 in the recipient FL are shown. The SNV was only detectable in the recipient FL. **D.** Quantitative PCR copy number assay at the *ARID1A* locus. The statistically significant decrease was confirmed in repeated iterations of this experiment. **E.** Immunohistochemistry for ARID1A/BAF250 (Santa Cruz) is shown in both lymphomas and a tonsil from a healthy individual. Figure S4B shows similar findings using a different anti-BAF250 antibody and normal control. **F.** SNVs in CTSS and ATP6V1B were detectable by Sanger sequencing only in the donor FL. Both were enriched in the DLI based on ultra-deep sequencing and CTSS M185V was also present in 4.7% of reads from the recipient's FL.

Author Manuscript Author Manuscript Author Manuscript Author Manuscript

Table 1

Summary of somatic mutations identified by exome sequencing, validated by Sanger sequencing and subjected to ultra-deep sequencing

Gene mutation	Exome sequencing		Sanger sequencing			Ultra-sensitive deep sequencing					final annotation
	cSNV/InDel frequency [% (variant/total reads)]		*confirmed*			*Donor leukocyte infusion*				*Nominal*	
	Donor's FL	*Recipient's FL*	*Donor's FL*	*Recipient's FL*	*DLI*	*Mutant reads*	*Mutant freq (×10²)*	*ratio to germline[a]*	*Enriched in DLI*	*p-value*	
BCL2 S203N	*13 (2/15)*	*30 (3/10)*	+	+	-	*68*	*0.14650*	*4.92*	+	*<10e-10*	*Identical mutations in both lymphomas*
BCL2 *206R	*20 (2/10)*	*0 (0/7)*	+	+	-	*95*	*0.16547*	*8.26*	+	*<10e-18*	
C10orf120 Q181H	*3 (1/31)[b]*	*50 (6/12)*	+	+	-	*1088*	*0.43355*	*3.99*	+	*<10e-134*	
CTSS M185V	*30 (14/47)*	*13 (1/8)[b]*	+	-[c]	-	*215*	*0.13062*	*1.75*	+	*<10e-7*	
EP300 V1148_F1149del	*15 (5/33)*	*27 (7/26)*	+	+	-	*628*	*0.09002*	*93.35*	+	*< 10e-15*	
GCLC R423K	*16 (6/19)*	*40 (4/10)*	+	+	-	*976*	*0.10818*	*3.71*	+	*<10e-94*	
GLI2 G1083R	*23 (2/13)*	*29 (2/7)*	+	+	-	*39*	*0.23376*	*3.46*	+	*<10e-4*	
GPR112 W71R	*19 (15/78)*	*28 (14/50)*	+	+	-	*1981*	*0.31435*	*4.77*	+	*<10e-282*	
GPR116 S494I	*13 (1/8)[b]*	*29 (4/14)*	+	+	-	*525*	*0.04489*	*6.34*	+	*<10e-67*	
HIST1H3G A115T	*16 (5/32)[b]*	*43 (6/14)*	+	+	-	*28*	*0.02315*	*≤1*	-	*NA*	
KLHL6 K485_T486insK	*18 (9/50)*	*21 (4/19)*	+	+	-	*147*	*0.03850*	*115.31*	+	*< 10e-15*	
SHANK2 R374Q	*24 (10/41)*	*33 (4/12)*	+	+	-	*458*	*0.69377*	*2.59*	+	*<10e-36*	
TAIP-2 V12A	*29 (16/55)*	*28 (7/25)*	+	+	-	*965*	*0.20534*	*3.94*	+	*<10e-133*	
TIGD6 C307Y	*21 (8/38)*	*22 (7/32)*	+	+	-	*1677*	*0.32210*	*3.48*	+	*<10e-177*	
TLN2 T588M	*17 (10/60)*	*21 (5/24)*	+	+	-	*416*	*0.26285*	*4.76*	+	*<10e-59*	
ATP6V1B2 R400Q	*19 (6/32)*	*0 (0/27)*	+	-	-	*655*	*0.08912*	*2.28*	+	*<10e-39*	*unique mutations in donor's FL*
RAFTLIN V254M	*28 (14/50)*	*0 (0/27)*	+	-	-	*19*	*0.04519*	*≤1*	-	*NA*	

Author Manuscript Author Manuscript Author Manuscript Author Manuscript

Gene mutation	Exome sequencing		Sanger sequencing		Ultra-sensitive deep sequencing					final annotation
	cSNV/InDel frequency [% (variant/total reads)]		*confirmed*		*Donor leukocyte infusion*				*Nominal*	
	Donor's FL	*Recipient's FL*	*Donor's FL*	*Recipient's FL*	*DLI*	*Mutant reads*	*Mutant freq (×10²)*	*ratio to germline[a]*	*Enriched in DLI*	*p-value*	
ARID1A R1276*	*0 (0/11)*	*60 (6/10)*	-	+	-[d]	*64*	*0.05055*	*≤1*	-	*NA*	*unique mutations in recipient's FL*
FGF23 A12T	*0 (0/3)*	*25 (2/8)*	-	+	-[d]	*152*	*0.05837*	*≤1*	-	*NA*	
HMCN1 T5167M	*0 (0/45)*	*16 (5/32)*	-	+	-[d]	*747*	*0.10826*	*≤1*	-	*NA*	
PLCE1 S1151T	*0 (0/45)*	*29 (4/14)*	-	+	-[d]	*51*	*0.00115*	*1.25*	-	*0.33*	

The Bonferroni adjusted two-sided p-value of 0.00238 was the level determining statistical significance. *NA*, not applicable;

[a] donor buccal swab served as germline;

[b] mutation initially not identified in filtered exome sequencing dataset (<2 variant reads or Phred Score <30) but subsequently recovered by visualization of reads using IGV (Integrated Genome Browser v2.0);

[c] not visible on Sanger sequencing of recipient's FL but present in 4.7% of reads by ultra-sensitive deep sequencing;

[d] mutations also not detectable in recipient buccal swab.